A Model of the β-AlFeSi to α-Al(FeMn)Si Transformation During Homogenization in 6xxx Alloys

Prepared by -- F. J. Vermolen, C. Vuik, and S. van der Zwaag, *Delft University of Technology, Delft, The Netherlands*,
N.C.W. Kuijpers, *Delft University of Technology, Netherlands Institute for Metals Research (NIMR), Delft, The Netherlands*
P.T.G. Koenis and K.E. Nilsen, *BOAL BV, de Lier, The Netherlands*

ABSTRACT --- One of the physical processes during the homogenization treatment of 6xxx aluminum alloys is the transformation of plate-like β-Al_5FeSi particles to more rounded shaped α-$Al_{12}(FeMn)_3Si$ particles. The rate of this transformation determines the homogenization time. Mathematically the β to α transformation is treated as a Stefan problem where the concentration and the position of the interfaces, separating the Aluminum phase and the α or β phase, have to be determined. The boundary conditions are obtained from thermodynamical calculations, using the ThermoCalc package. A Finite element model and an analytical model, which mimic the growth of an α particle on a dissolving β plate, are proposed and compared. Finally, some metallurgical implications are given.

INTRODUCTION

The phase transformation of β-AlFeSi to α-Al(FeMn)Si is an important process during the homogenization of cast AA 6xxx aluminum alloys. During this homogenization process, at temperatures between 530-600°C,[1] plate-like monoclinic intermetallic β-Al_5FeSi particles transform to multiple rounded α-$Al_{12}(Fe_xMn_{(1-x)})_3Si$ particles[2-4]. This phase transformation improves the processability of the aluminum considerably. The plate-like β-particles can lead to local crack initiation and induce surface defects on the extruded material. The more rounded α-particles in the homogenized material improve the extrudability of the material and improve the surface quality of the extruded material.[5,6] Additional processes, such as the dissolution of Mg_2Si particles also occur during homogenization. Since the Mg_2Si particles dissolve rather quickly, the β→α transformation kinetics determine the minimum time that is needed to get a good extrudability.[7] Many process parameters, such as homogenization temperature,[8] as-cast microstructure,[9] and chemical compostion[10] influence the transformation rate.

The morphological change of the intermetallics during the homogenization treatment has been described in a few papers. In the early stage of transformations it was found that α particles were nucleated on top and also on the rim of the β-plate.[11,12] Small α nuclei, with an average size of half a micrometer, are observed on top of the β particles with a site density of approximately 0.2 μm^{-2}. Some of the particles observed were facetted whereas others exhibited a more rounded morphology. During the transformation, the β-AlFeSi phase is observed to remain plate-like with an approximately constant thickness,[4] leading to the conclusion that the β plate only dissolves at the rim, injecting Fe and Si into the Al-matrix. From TEM and SEM experiments, it is observed that the interface between the α-particle and β-plate does not move.[13] Hence, there is no mass transport across the interface between the α-particle and β-plate. Since the α particles grow by adsorption of Si, Mn and/or Fe, those elements must have been transported through the Al-matrix.

Until now, no physically based models have been found in the literature which predict the fraction transformed of the β to α transformation. Hence, modeling this transformation and looking at the influence of the process parameters poses a new challenge.

In this paper, a model is proposed based on the hypothesis that the transformation is diffusion

controlled. The transformation is mathematically treated as a Stefan problem,[34] where the concentration satisfies the diffusion equation and the position of the moving boundaries was determined from conservation of mass. This model can only be used in the beginning of the transformation. The reasons for this are: firstly, in the beginning the overall morphology is still stable, whereas the intermetallics break up to cylindrical shapes at later stages. Secondly, if the dissolving β-rim meets the growing α-particle, our model is no longer applicable. Despite this limitation, the model could provide some idea of the homogenization-time towards higher fractions (up to approximately 50 percent).

In this paper, a finite element and an analytical approach are presented which model the development of fraction transformed with time, by simulating the growth of an α particle on a β plate. For the boundary conditions of the model, thermodynamic calculations are used (Thermo-Calc). The transformation fraction is calculated for several input parameter values estimated from experimental observations. The influence of some process parameters on the transformed fraction, such as the temperature and initial thickness of the β plates, are investigated in [34]. The finite element model and the analytical model are compared, and finally the model is validated with experimental data. The dependence of the transformation rate on the alloy content such as Mn and Si is also an important implication of the model, and will be described in more detail in [25].

THE TRANSFORMATION MODEL

In our model, a solubility difference between the α interface and the β-interface rim gives a mass transport of Si and Fe through the Al matrix between the two phases. This leaves the α particle to grow and the β plate to dissolve.

For the present study only a uniform initial (at *t=0*) composition of the Al-rich phase is considered. It is assumed that the atoms of the alloying elements diffuse through the Al-rich phase. Further, atoms that originate from the α- and β-phase are assumed to cross the interface (α/Al phase or β/Al phase) at such a rate that bulk diffusion is the rate-controlling step in the transformation. From mass-conservation a Stefan problem results to determine the movement of the interface. Further based on experiments, we assume that the β plate only dissolves at its rim and the face of the β plate is unaffected. The initial matrix concentrations are determined from the Scheil model. We further assume that Si is uniform in the Al matrix. The rate of the transformation is assumed to be determined by diffusion of Fe. Alexander et al.[27] found that Mn diffusion is only a secondary effect on the transformation and hence it hardly controls the speed of the transformation. This is due to the low diffusivity of Mn. A final assumption is that the stoichiometries of the α and β phases are fixed during the transformation. For the determination of the interfacial concentrations, we use ThermoCalc and the multi-component model. Here the interfacial concentrations are determined such that the interface velocity is the same for all the alloying elements and such that the interface concentrations satisfy a solubility product. More details on the model are presented in [34].

Model Geometry

For 6xxx alloys the α phase is stable with respect to the β phase. The nucleation of α-particles takes place preferentially on the β/Al interface rather than in the aluminum matrix, since the activation energy for nucleation of α particles on the β/Al interface is lower[29] than the nucleation energy in the Al-matrix. Therefore our model considers only this heterogeneous nucleation of α-particles on the β/Al surface. Experimentally, a distribution of nucleation distances was found, but for the sake of simplicity we only take the mean nucleation distance as model input parameter.

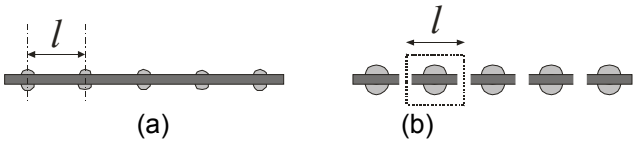

Figure 1. A scheme of (a) an β plate with initial α nuclei in the non-homogenized state (b) A broken β plate with consisting α particles on top. The domain of computation is situated in the picture.

The average plate length of the initial β-particles is approximately 20 μm, and the average nucleation distance is approximately 2 μm. It was found by experiment that β particles break up and transform to α-particles. Yet, it is not clear how the β plate breaks up during the transformation. In our model we propose that the β particles break up with the same length as the nucleation distance. This is illustrated in Figure 1. Figure 1a shows an initial β plate with α nuclei. Figure 1b shows the situation after a short homogenization time: The β plate breaks up, and the α particles start to grow. The domain of computation is indicated by the dotted box.

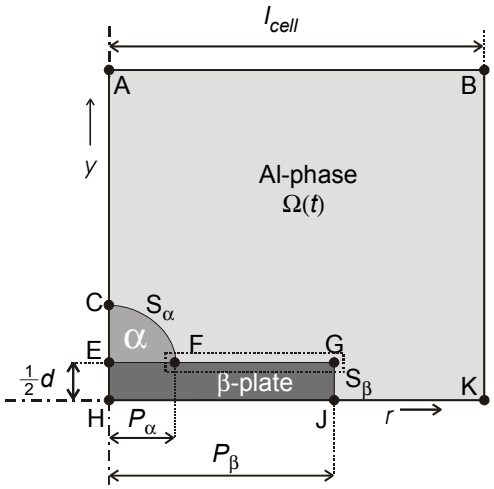

Figure 2. The geometry of the domain of computation of an α-particle on a β-plate in an Al-phase. The parameters are explained in the text.

Figure 2 shows the geometry of the model that mimics the growth of an α-particle on a dissolving β-plate.

The as-cast microstructure is simplified in the Finite Element Model to a representative cell containing the Al-rich phase, a single α particle and a single β-plate, which have a specific form and size. Furthermore, the cell size is chosen such that diffusion across cell boundaries is negligible. In the FE-Model we calculate a cell area with the size of $l_{cell} \times l_{cell}$. We assume cylindrical symmetry around the left vertical axis. A hemispherical α particle is situated on top of the plate-like β particle, and has a distance towards the rim of the β particle. The drawing is only schematic as the dimensions are not properly scaled according to those used in the calculations.

The aluminum phase is indicated in Figure 2 by the domain Ω(*t*), in which diffusion of the alloying elements takes place. The time dependence of this domain is induced by the moving boundaries of the α-particle and the β-plate. Those moving boundaries are expressed by the segment CF, defined as S_α, and the line segment GJ, defined as S_β. The unit normal vectors at the interfaces S_α and S_β, pointing outward from the aluminum matrix, are denoted by $\mathbf{n}_\alpha$ and $\mathbf{n}_\beta$ respectively. Since the β face is unaffected the line segment, FG does not move.

Line segment HK represents a symmetry line. Therefore the presented thickness of the β-plate in Figure 2 is only half of the modeled thickness of the β-plate, *d*. During this transformation this thickness remains constant, as also stated in assumption 1. Line segment AH represents the second symmetry line. For the Finite Element model, cylindrical co-ordinates are used, where the α-particle represents a hemispherical shape and the β plate represents a disc-like shape in three dimensions. In the case of planar coordinates the α-particle represents an hemi-cylindrical shape and the β plate represents a rectangular shape in three dimensions.

The Finite Element Model

The Finite Element Model (FEM) is based on the solution of Fick's second law for diffusion in two dimensions. Further, a mass conservation of argument leads to the Stefan condition, where the normal component of the interface velocity is proportional to the concentration gradient. On the fixed boundaries the normal derivative of the concentration field is zero. A more detailed description of the model is presented in [34].

The presented mathematical problem has been implemented in the package SEPRAN, which has been developed at the Department of Applied Mathematical Analysis at the Delft University of Technology. The resulting discretized Stefan problem is solved by the use of a moving grid method, where the grid is adjusted according to the interface movement. The interface movement is determined in a conservative way. The method is described in detail by Segal et al. [30].

In the calculations it is assumed that the initial α-particle is spherical with radius r_α^{init} and that the initial β-plate is cylindrical with radius *l*. The Gibbs-Thomson effect only has a significant influence on the transformation kinetics when the radius of curvature is very small (typically in the order of nanometer). Since we consider only transformation behavior in a micrometer-scale, we neglect the Gibbs-Thomson effect in the computations.

Analytical Approach

The analytical approach is based on the assumption that diffusion in the horizontal direction (i.e. the r-direction) only plays a role (see Figure 2). To justify this, we show the concentration field, *c(r,y,t)*, in the aluminum matrix in the vicinity of the interfaces in Figure 3. As the variation of the concentration in the vertical direction close to the β plate is very small, it is reasonable to assume that there the second derivative in the y-direction is

negligible. This motivates the one-dimensional approach. Just as in the FEM calculations, the analytical model is based on volume diffusion, where only diffusion close to the β-plate is considered, such that a one-dimensional Stefan problem arises. A further assumption is that the time dependence in the diffusion equation is negligible. We summarize this as follows:

Main Assumptions of the Analytical Model

1. The growth of the α- and β–phases is determined by the derivation of the growth of the interface position of the α particle at the triple point F, and the rim point G of the β-plate (Figure 2).

2. The rate of interface movement is very small compared to the rate of diffusion in the α-matrix (steady state assumption).

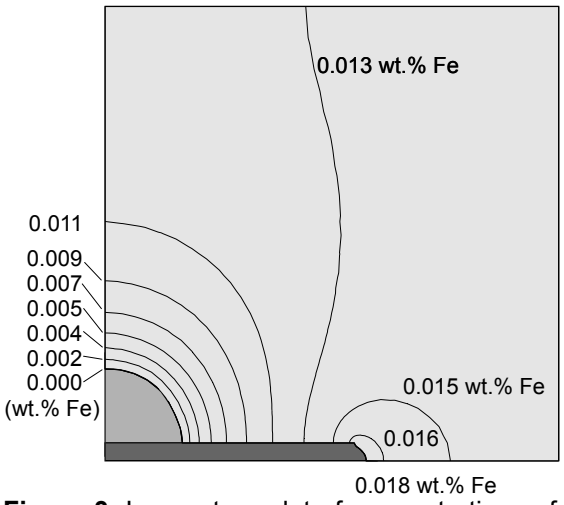

Figure 3. Iso-contour plot of concentrations of Fe in a cylindrical symmetric situation on an alloy homogenized for 60 minutes at 580 °C, as obtained by FEM calculations. The model parameters are presented in Table 1.

A consequence of the assumptions is that we have on the β plate surface between the points F and G

$$\frac{D}{r}\frac{\partial}{\partial r}\left(r\frac{\partial c}{\partial r}\right)=0, \qquad (1)$$

where the concentrations at F and G serve as boundary conditions.

For its tractability we only treat the rectangular case here. The cylindrical case is dealt with in a similar manner. Combined with the boundary conditions at the moving interfaces the solution of the above equation is:

$$c=\frac{c^{sol}{}_{\beta}-c^{sol}{}_{\alpha}}{P_{\beta}-P_{\alpha}}(r-P_{\alpha})+c^{sol}{}_{\alpha}.$$

The Stefan condition for both moving interfaces reads as:

$$\frac{dP_{\alpha}}{dt}=\frac{D}{c^{part}{}_{\alpha}-c^{sol}{}_{\alpha}}\frac{\partial c}{\partial r}(P_{\alpha},t)$$
$$\frac{dP_{\beta}}{dt}=-\frac{D}{c^{part}{}_{\beta}-c^{sol}{}_{\beta}}\frac{\partial c}{\partial r}(P_{\beta},t)$$

Combination of the expressions in the above equations with the solution gives after integration:

$$P_{\alpha}(t)-P_{\alpha}(0)=\frac{c^{part}{}_{\beta}-c^{sol}{}_{\beta}}{c^{part}{}_{\alpha}-c^{sol}{}_{\alpha}}(P_{\beta}(0)-P_{\beta}(t))$$

After some elementary algebra this will give equations for the interface positions. We see that the collision time t_{col} is proportional to the square of the initial distance between the reminiscent phases, $P_{\beta}(0)-P_{\alpha}(0)$:

$$t_{col}=\frac{(P_{\beta}-P_{\alpha})^2}{2(c^s_{\beta}-c^s_{\alpha})D_{Fe}\left((c^p_{\alpha}-c^s_{\alpha})^{-1}+(c^p_{\beta}-c^s_{\beta})^{-1}\right)}$$

The analytical solutions are compared with the FEM solutions in the section of the discussion and results.

EXPERIMENTAL DETAILS

An Al-Mg-Si alloy (AA 6005 A) with an alloy composition of 0.70 wt.% Mg, 0.83 wt.% Si, 0.27 wt.% Fe, and 0.18 wt.% Mn has been used for our investigations. All other chemical elements were present in weight percentages of at most 0.01 wt.%, hence their presence is ignored. The investigated alloy was DC-cast with a diameter of 254 mm.

To investigate the β→α transformation rate, series of samples were homogenized at temperatures of 540°C, 570°C and 580°C for various times ranging between 10 minutes and one day. The samples were homogenized in an air circulation oven, for which the maximum temperature deviation over all locations is 3 °C. The samples were taken

from the billet at locations between 10 mm and 30 mm from the rim of the billet. The microstructure of these samples, represent the typical microstructure of the billet. The experimental relative α-fraction was determined by using automatic SEM measurements in combination with Electron Dispersive X-ray Spectography (EDX). The α- and β- particles are classified by the difference of stoichiometric ratio of the total concentration of Fe and Mn versus the concentration of Si, which is determined by EDX. The method is described in more detail in [7].

At different distances of 20 mm, 50 mm and 75 mm from the rim of the billet, the mean dendrite arm spacing (DAS) has been determined. Each DAS value was determined by averaging 50 separate DAS-spacings determined from five optical micrographs on the same polished sample.

The samples were polished with one-fourth silica and subsequently electro-etched at 20 V during 30 seconds in a mixture of 78 perchloric acid, 90 mL water, 730 mL ethanol and 100 mL butylglycol. SEM micrographs (JEOL 6500F) of these samples were used to measure the mean thickness of the β-plate. The thickness of the β-plates was determined by the use of SEM micrographs by averaging 50 individual thicknesses. The true thickness in 3-D was taken to be π/4 times the average thickness from the cross section images.

The nucleation distance between individual α particles was measured on two fully homogenized samples, either homogenized for 32 hours at 590 °C, or homogenized for 130 hours at 540°C. Each sample was polished with one-fourth Silica. Subsequently 20 optical micrographs were made on each sample. The distance between neighbouring α particles (*l*), which were located along a former β-plate, was determined by the use of the sketch of Figure 4. The nucleation distance in polished plain is obtained from *L*/(n-1), where *L* represents the distance between the outside particles, and n is the number of particles on a sequence. The median nuclei distance, was determined by the use of 20 measurements of α-particles. The true nuclei distance in 3D, *l*, was taken to be one half times the median nuclei distance from the measurements.

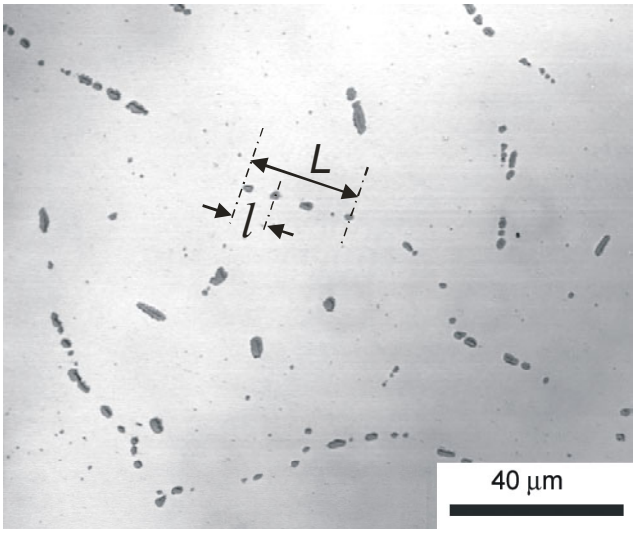

Figure 4. Microstructure of the fully homogenized sample at 590°C. The method of the determination of the distances between the beads of the α particles on the former β plate is showed.

RESULTS AND DISCUSSION

In this section, first the analytical model will be compared with the results of the FEM model. Then, the experimental results will be compared with the results obtained by the mathematical models. Finally the metallurgical implications will be given. A detailed parametric study is presented in [34] and [25], where the influence of the temperature, initial concentrations, initial sizes of the α and β phases on the transformation rate is investigated.

The simulation is done for an industrial temperature of 580°C, therefore the reported parameters are also obtained for this temperature (Table 1). We used the literature values of the densities of Al, α and β phases[31] for the derivations of the concentration of Fe inside the α and β particles.

The Scheil[26,29] model derives the initial concentration of different elements in the Al-matrix close to the intermetallics. Since the FEM cell is relatively small compared to the DAS, and is situated close to the intermetallics, it is assumed that the initial concentration is homogeneously distributed in this FEM cell and is equal to the derived concentrations. By Scheil calculations in Thermo-Calc, which use the compositions of the experimental alloy as input, initial concentrations were found of c_{Fe}^{0}=0.02 wt.%,

c^0_{Mg} = 0.6 wt.%, c^0_{Si} = 0.5 wt.% and c^0_{Mn} = 0.25 wt.%.

The concentrations on the interface of the β particles are determined by the multi-component model. The procedure is described in [34]. The geometric parameters, as presented in Table 1, are estimations from previous research.[4,12]

Table 1. Basic Physical Parameters Used for the Model

Parameter	Symbol	Value
Diffusion coefficient (at T=580°C)	D_{Fe}	0.0307 μm^2/s
Fe concentration in α particle [**31**]	c^p_α	39.9 wt.%
Fe concentration in β particle [**31**]	c^p_β	33.9. wt.%
Fe content on interface of α particle	c^s_α	0 wt.%
Fe content on interface of β particle	c^s_β	0.0183 wt.%
Initial radius of α particle	r^{init}_α	0.25 μm
Thickness of β-plate	d	0.2 μm
Diameter of initial β-plate	l	3 μm
Cell size of aluminum matrix	l_{cell}	2.5 μm
Initial iron concentration in matrix	c^0_{Fe}	0.0200 wt.%
Temperature	T	580°C

Comparison Between Both Approaches

Figure 5 shows the evolution of the relative α-fraction, fα, for the analytical, and FEM model, for both cylindrical and planar symmetry. For the analytical approach it is assumed that the α particle stays rounded during the transformation, and its radius is defined by the position of the triple point F. Figure 5 shows that for the calculation of the relative α-fractions in the early stage, the analytical model is a reasonable alternative to the FEM calculation. For later stages (higher than $f_\alpha \approx 0.40$) the differences become too large.

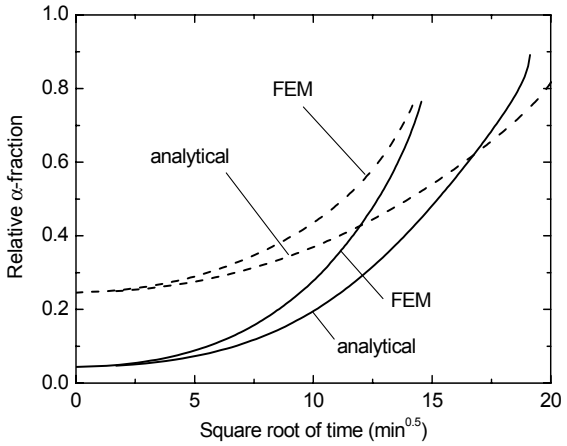

Figure 5. The evolution of the relative α-fraction by the use of the analytical approach and by the use of FEM, for cylindrical (as denoted by the straight lines) and planar (as denoted by the dashed lines) symmetry. The model parameters are presented in Table 1.

Model Versus Experiments

In the previous sections, we showed that the model showed realistic characteristics. In this section we want to perform a more quantitative comparison of the model calculations versus experiments. For the model calculations a cylindrical geometry is used with geometrical dimensions as experimentally determined. All other parameters are as presented in Table 1.

The mean thickness of the initial β-plate had a median thickness of 0.2 μm. This thickness of the β plate had a wide natural variation with a standard deviation of 0.15 μm. We did not find a statistically significant change in the mean thickness at later stages of homogenization (f_α≈0.2 and f_α≈0.5). This supports the hypothesis that the thickness does not change during the homogenization. Note that the thicknesses, found by SEM, are somewhat smaller than the thickness found by optical microscopy in [4] because SEM measurements also detect thinner β particles, which are not visible for optical microscopy. For the sake of simplicity, in this model we only consider the median thickness in calculations.

The nucleation distance of the α particles was determined. For the fully homogenized sample at 540°C the median distance was equal to 1.75 μm, and for a fully homogenized sample at 590°C this distance equals approximately 1.5 μm. There is a

wide natural variation of the nucleation distances, with a standard deviation of 0.5 μm, but for the sake of simplicity, in this model we only take the nucleation density l=1.5 μm as a model parameter, and we neglect the temperature dependence. Note that although the median nucleation distances were corrected for the 3D situation, the values still fall within the measured distribution of the nucleation distances in the 2-D plane.

The average DAS was approximately 20 μm. In the numerical calculations, we found that the cell size hardly has any influence on the numerical results providing it is larger than the β plate. Therefore, to reduce the computational effort, we used a numerical cell size which is smaller than the dendrite arm spacing, l_{cell} = 2.5 μm.

The morphology assumed in the model calculations was also validated against some SEM micrographs. In [34] we present some SEM micrographs of an α particle growing on top of a β plate. The morphology corresponds well with the FEM calculations. The micrographs also show that the α particle does not stay spherical during growth. The same behavior is observed for the FEM calculations. Secondly, the micrographs reveal that the interface between the α and β phases remains in its place.

Figure 6 shows the relative α-fraction as a function of time computed by FEM and experiments. The time and temperature dependence of the relative α-fraction of the FEM model agrees well with the experiments. It should be pointed out that the model is capable of predicting the transformation fraction up to approximately f_α=0.5.

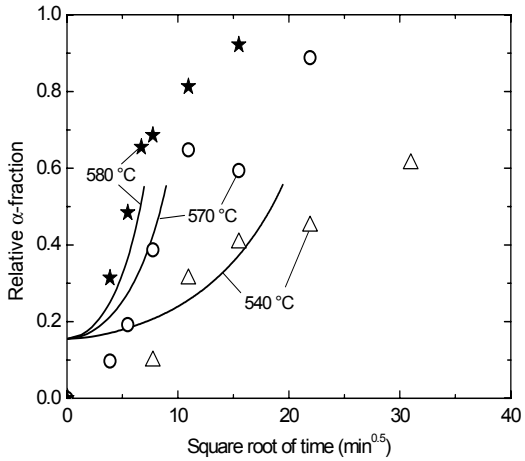

Figure 6 The relative α-fraction as a function of time derived by the Finite Element Model (presented by the straight lines) compared with the relative α-fractions, measured by experiments (presented by the separate points). The calculations and measurements are performed for three different temperatures.

Metallurgical Implications

A proper homogenization leads to a considerable increase in the extrudability and leads to fewer surface defects on the aluminum profiles. Therefore, an extrusion ingot is homogenized to attain a high relative α fraction, e.g., at least f_α=0.8 and preferably more than f_α=0.9.[1] Although the presented transformation model is not applicable to homogenization up to high relative α-fractions, still some important metallurgical implications can be extrapolated from the numerical experiments.

Three aspects influence the homogenization process in particular: the homogenization temperature, the morphology of the intermetallics, and the alloy content.

A high temperature dependence of the transformation rate was found in [34], both for numerical and experimental results. Industrial homogenization temperatures of extrusion ingots are typically at approximately 585ºC.[1] The model showed that a decrease of the homogenization temperature of, e.g., 5ºC leads to a considerable increase of the required homogenization time of approximately 20 percent. Therefore, accurate temperature control is a very important aspect to achieve efficient homogenization.

The morphology of the intermetallics has an important effect on the transformation speed. A parameter study in [34] indicates that thin β-particles will transform faster than thick β particles. Therefore it is important that the as-cast structure contains more thinly distributed β particles, to achieve fast homogenization times. Grain refinement, alloy composition, and cooling speed mainly determine the coarseness of the β-AlFeSi particles, and therefore those parameters have to be optimised.

The effect of the DAS was also investigated on the transformation speed. Experiments on the studied AA 6005A alloy indicates that the DAS ranges between 19 μm and 23 μm, within the DC-cast billet. The results as given in [34] indicate that this slight variation in DAS does not lead to a significant effect on the transformation speed. The influence of the alloy composition was not investigated in this study and will be discussed in [25]. The model implies that Mn concentrations higher than 0.10 and Si concentrations lower than 0.3 wt % increase the transformation speed.

CONCLUSION

A Finite Element Model has been presented which describes the initial stages of the β-AlFeSi to α-Al(FeMn)Si transformation. The model predicts a strong effect of temperature and intermetallic morphologies on transformation kinetics. In spite of major simplifications in initial morphologies of the intermetallics, the calculated FEM results agree over a large range of temperatures, with experimental data. A simple analytical model yielded qualitatively the same behavior, however, its quantitative agreement is rather poor. We conclude from the good agreement of the FEM calculations and experiments that the β→α phase transformation kinetics is diffusion controlled.

ACKNOWLEDGEMENTS

We thank J.P. Mulder for the DAS measurements.

REFERENCES

[1] Parson, N. C., J. D. Hankin, K. P. Hicklin: *Al-Mg-Si Alloy with Good Extrusion Properties*, US-pattent (2002) 6, 440, 359.

[2] Zajac, S., B. Hutchinson, A. Johansson, and L. O. Gullman: *Mat. Sci. Tech*. 10, (1994) 323-333.

[3] A. Valles, R., P. L. Orsetti, and R. Tosta: *Proceedings of the International Conference on Aluminium Alloys,* (Toyohashi, Japan, 1998) 2123-2128.

[4] Kuijpers, N. C. W., J. Tirel, D. N. Hanlon, and S. van der Zwaag: *Mat. Char*. 48 (2002) 379-392.

[5] Clode, M. P. and T. Sheppard: *Aluminium Technology '86, The Institute of Metals, 1 Carlton House Terrace*, London SW1Y 5DB, UK, 1986, pp. 230-239.

[6] Minoda, T., H. Hayakawa, and H. Yoshida: Mater. Sci. Techn. **7** (2000) 13-17.

[7] Kuijpers, N. C. W., W. H. Kool, P. T. G. Koenis, K. E. Nilsen, I. Todd, and S. van der Zwaag: *Assessment of Different Techniques for Quantification of Intermetallics in AA 6xxx alloys*, accepted for publication in Mat. Charact. 2003.

[8] Onurlu, S. and A. Tekin: J. Mat. Sci. 29 (1994) 1652-1655.

[9] Tanihata, H., T. Sugawara, K. Matsuda, and S. Ikeno: *J. Mat. Sci.* 34 (1999) 1205-1210.

[10] Lamb, H. J.: *Proceedings of the Conference on Phase Transformations,* (London, England, 1979) Series 3, No. 1, 2, V4-V5.

[11] Lodgaard, L. and N. Ryum: *Mat. Sci. Eng. A* 283 (2000) 144-152.

[12] Kuijpers, N. C. W., J. Tirel, D. N. Hanlon and S. van der Zwaag: *On the characterisation of the α-Al(FeMn)Si Nuclei on β-AlFeSi Intermetallics by Laser Scanning Confocal Microscopy*, send for publication in *J. of Mater. Sci. Let.*

[13] Kuijpers, N. C. W. and S. v.d. Zwaag: "*Observations of α-Al(FeMn)Si Nuclei on β-AlFeSi Intermetallics by SEM and TEM*", to be send for publications in *J. of Mater. Sci.*

[14] J. Crank: *Free and moving boundary problems*, (Clarendon Press, Oxford, 1984).

[15] M. J. Whelan*: Metal. Sci. J*. **3** (1969) 95-97.

[16] Aaron, H. B. and G.R. Kotler: *Metall. Trans*. A 2 (1971) 393-408.

[17] Tundal, U. H. and N. Ryum: Metall. *Trans. A 23* (1992) 433-444.

[18] Reiso, O., J. Strid, and N. Ryum: Metall. *Trans. A 24* (1993) 2629-41.

[19] Hubert, R.: *ATB Metallurgie* 34-35 (2002) 4-14.

[20] Vitek, J. M., S. A. Vitek and S. A. David. *Metall. Trans.* A 26 (1995) 2007-2025.

[21] Vermolen, F. J. and C. Vuik. J*: Comput. Appl. Math.* 126 **(**2000) 233-254.

[22] Vermolen, F. J., C. Vuik, and S. van der Zwaag: *Mater. Sci. Eng*. A 328 (2002) 14-25.

[23] Kobayashi, R.: *Physica* D 63 (1993) 410-23.

[24] Grafe U., B. Bottger, J. Tiaden, and S. G. Fries: *Scripta Mater*. 42 (2000) 1179-86.

[25] Kuijpers, N. C. W., P. T. G. Koenis, K. E. Nilsen, F. Vermolen, C. Vuik and S. v.d. Zwaag, "Alloy Dependence of the β-AlFeSi to α-Al(FeMn)Si Transformation Kinetics in Al-Mg-Si alloys," in progress, 2003.

[26] Scheil, E.: *Z.Metallkd* 34 (1942) 70-72.

[27] Alexander, D. T. L. and A. L. Greer: *Acta Mater.* 50 (2002) 2571-83.

[28] Fujikawa, S., K. I. Hirano, and Y. Fukushima: *Metall. Trans*. A 9 **(**1978) 1811-1815.

[29] Porter, D. A. and K. E. Easterling: *Phase Transformations in Metals and Alloys*, (Chapman & Hall, London, 1997).

[30] Segal, G., C. Vuik, and F. J. Vermolen: *J.Comp. Phys.* 141 (1998) 1-21.

[31] Mondolfo, L. F.: *Structure and Properties of Aluminium Alloys*, (Butter-worth, England, 1976).

[32] Belov, N. A., A. A. Aksenov, and D. G. Eskin: *Iron in Aluminum Alloys, Impurity and Alloying Element,* (Taylor & Francis, London and New York, 2002) 132-136.

[33] Beke, D. L., I. Gödény, I. A. Szabó, G. Erdélyi, and F. J. Kedves: *Philos. Mag*. A **5** (1987) 73-78.

[34] Kuijpers, N.C.W., F.J. Vermolen, C. Vuik, and S. Van der Zwaag: *Mater. Trans*. 44 (7) (2003) 1448-1456.